Polyamine-Substituted Gadolinium Chelates: A New Class of Intracellular Contrast Agents for Magnetic Resonance Imaging of Tumors

Markus Wolf,[†] William E. Hull,[‡] Walter Mier,[§] Sabine Heiland,[||] Ulrike Bauder-Wüst,[†] Ralf Kinscherf,[⊥] Uwe Haberkorn,[§] and Michael Eisenhut[†,*]

Department of Radiopharmaceutical Chemistry, German Cancer Research Center (DKFZ), Im Neuenheimer Feld 280, D-69120 Heidelberg, Germany, Central Spectroscopy Department, German Cancer Research Center (DKFZ), Im Neuenheimer Feld 280, D-69120 Heidelberg, Germany, Department of Nuclear Medicine, University of Heidelberg, Im Neuenheimer Feld 400, D-69120 Heidelberg, Germany, Division of Experimental Neuroradiology, University of Heidelberg, Im Neuenheimer Feld 400, D-69120 Heidelberg, Germany, and Institute for Anatomy and Cell Biology, University of Heidelberg, Im Neuenheimer Feld 307, D-69120 Heidelberg, Germany

Received August 21, 2006

A new class of intracellular contrast agents (CA) for magnetic resonance imaging has been developed, based on Gd(DTPA) with two positively charged amide-linked substituents. Uptake of Gd(DTPA) into cultured tumor cell lines (B16 mouse melanoma, MH3924A Morris hepatoma) was below the detection limit while CA with the melanin-binding pharmacophore 2-(diethylamino)ethylamine reached intracellular concentrations of ca. 0.03 fmol/cell (ca. 20 μM) for melanoma and 0.02 fmol/cell for hepatoma (24 h at 10 μM CA). With the polyamine substituents bis(2-aminoethyl)amine or spermidine, CA uptake increased up to 3-fold for melanoma (0.083 fmol/cell) and 9-fold for hepatoma (0.18 fmol/cell). Uptake of polyamine-substituted CA was reduced by the polyamine transport inhibitor benzyl viologen. Molar relaxivities for three Gd-DTPA-polyamine complexes were in the range 5.6−6.9 for the free complex in solution and 7.7−23.5 s^{-1} mM^{-1} for Morris hepatoma cell pellets. T_1-weighted magnetic resonance imaging at 2.35 T of rats with MH3924A tumors showed contrast enhancement in tumor at 1 and 24 h postinjection of polyamine-substituted CA.

Introduction

To enhance magnetic resonance imaging (MRI[a]) contrast between normal and pathological tissue or between specific tissue compartments, a variety of intra- or extravascular paramagnetic contrast agents (CA) are available, e.g., extracellular agents such as the gadolinium(III) chelation complex Gd-(DTPA) ([Gd(DTPA)(H_2O)]$^{2-}$; DTPA = diethylenetriamine-*N*,*N*,*N*′,*N*″,*N*″-pentaacetic acid) or Gd(DO3A-butrol) ([Gd(DO3A-butrol)(H_2O)]; DO3A-butrol = 1,4,7-tris(carboxymethyl)-10-(1,2,4-trihydroxy-but-3-yl)-1,4,7,10-tetraazacyclododecane).[1] By increasing the relaxation rate $R_1 = 1/T_1$ of neighboring water protons in the vasculature or interstitium, such agents enhance the intrinsic contrast between tissues or compartments in T_1-weighted MR images in a concentration-dependent manner.

Increasing efforts are being made to develop target-specific agents.[2−5] For example, tissue specificity has been achieved with complexes conjugated to monoclonal antibodies.[6,7] As an alternative, folate dendrimer-based contrast agents have been developed which bind to the high-affinity folate receptor (hFR) overexpressed in many types of epithelial tumors such as ovarian carcinomas.[8] However, the number of cell-surface antigens or receptors that can be utilized by extracellular, interstitial contrast agents may represent a limitation of this technique.

Another interesting strategy is to employ *intracellular* uptake as a means of "labeling" the cells of interest, whereby 10^7−10^8 Gd(III) complexes (0.017−0.17 fmol) per cell need to be internalized to achieve a detectable contrast enhancement via T_1-weighted MRI. Ideally, CA uptake should reflect a specific tissue type or pathophysiologic process of diagnostic significance. However, only a few reports have appeared concerning cellular internalization of gadolinium complexes, which may be attributed to the lack of specific transporters for the currently used CAs.[8−11] Intracellular MRI CAs employing membrane-penetrating peptides, such as the arginine-rich HIV-tat membrane translocation signal peptide[11,12] or polyarginine oligomers,[9] lack tissue (e.g., tumor) selectivity.[13] Stem cells can internalize [Gd(HP-DO3A)(H_2O)] by pinocytosis and have been labeled with this agent in ex vivo incubations.[14] Gd-texaphyrin, a porphyrin-based agent, exhibits tumor cell uptake[15] with rapid influx and efflux characteristics.[16] To our knowledge, there have been no reports of an intracellular CA which can serve as a marker for tumor cells in general or for a specific tumor type such as melanoma.

The pharmacophores *N*-(2-diethylaminoethyl)benzamide and 2-(diethylamino)ethyl-carboxamide enhance the intracellular delivery of a series of technetium metal complexes.[17−19] The 2-diethylaminoethyl side chain was found to be responsible for targeting of benzamide derivatives to melanoma cells.[20−23] High melanin affinity was also found for spermidine-substituted benzamides[24] or the polyamines themselves.[25] It has been suggested that the radioiodinated benzamides used for melanoma scintigraphy enter tumor cells not only by passive diffusion but also by active transport via polyamine carriers.[26] Biogenic

* To whom correspondence should be addressed. Phone: +49-6221-42-2443. Fax: +49-6221-42-2431. E-mail: m.eisenhut@dkfz.de.

[†] Department of Radiopharmaceutical Chemistry, German Cancer Research Center (DKFZ).

[‡] Central Spectroscopy Department, German Cancer Research Center (DKFZ).

[§] Department of Nuclear Medicine, University of Heidelberg.

[||] Division of Experimental Neuroradiology, University of Heidelberg.

[⊥] Institute for Anatomy and Cell Biology, University of Heidelberg.

[a] Abbreviations: DO3A-butrol, 1,4,7-tris(carboxymethyl)-10-(1,2,4-trihydroxy-but-3-yl)-1,4,7,10-tetraazacyclododecane); DTPA, diethylenetriamine-*N*,*N*,*N*′,*N*″,*N*″-pentaacetic acid; HP-DO3A, 1,4,7-tris(carbonylmethyl)-10-(2′-hydroxypropyl)-1,4,7,10-tetraazacyclododecane; Boc, *t*-butyloxycarbonyl; DO3A, 1,4,7,10-tetraazacyclododecane-1,4,7-triacetic acid; DOTA, 1,4,7,-10-tetraazacyclododecane-1,4,7,10-tetraacetic acid; DTPA, diethylentriamminpentaacetic acid; DTPA-BMA, diethylenetriamine-*N*,*N*′,*N*″-triacetic acid-bis-*N*,*N*″(methyl)amide; HIV, human immunodefficiency virus; ICP−MS, inductively coupled plasma mass spectrometry; MRI, magnetic resonance imaging; MTS, (3-[4,5,dimethylthiazol-2-yl]-5-[3-carboxymethoxy-phenyl]-2-[4- sulfophenyl]-2*H*-tetrazolium, inner salt; TLC, thin layer chromatography; TSP, trimethylsilyl propanoic acid; TFA, trifluoroacetic acid.

10.1021/jm061003a CCC: $37.00
Published on Web 12/16/2006

Chart 1

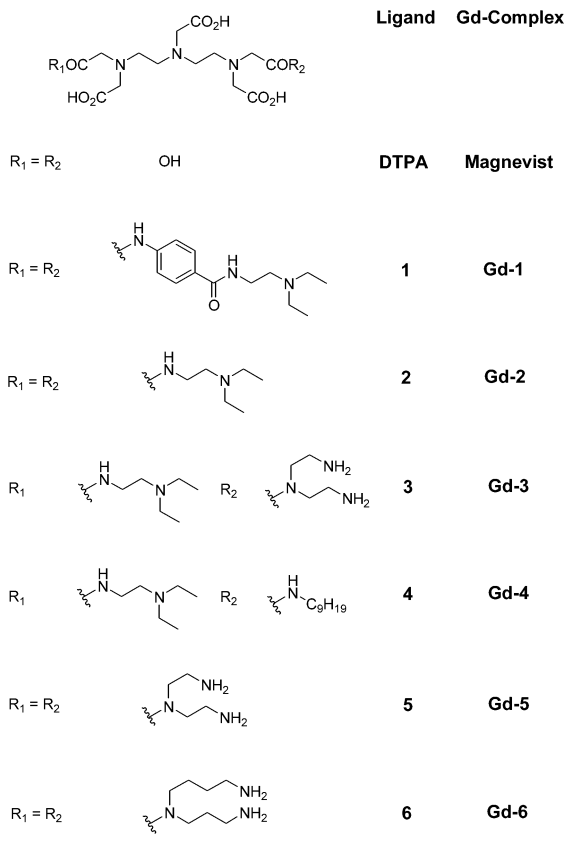

polyamines (putrescine, spermidine, spermine) are internalized by receptor-mediated active transport processes which can result in the accumulation of up to millimolar quantities with intra-to-extracellular ratios of polyamines as high as 1000.[27,28] Furthermore, when cell proliferation is stimulated, polyamine uptake increases relative to that in nonproliferating tissue.[29]

The primary objective of this work was to determine whether or not basic amine substituents such as the known melanoma-seeking pharmacophores or polyamines are able to facilitate intracellular uptake and retention of gadolinium-DTPA complexes in tumor cells and elicit melanoma-targeting behavior. Therefore, we investigated the pharmacophores 4-amino-*N*-(2-diethylaminoethyl)benzamide (procainamide) and 2-(diethylamino)ethylamine as well as the bacterial polyamine bis(2-aminoethyl)amine[30] and the mammalian polyamine *N*-(3-aminopropyl)-1,4-diaminobutane (spermidine) as DTPA substituents (Chart 1). The polyamine transport system has broad substrate tolerance,[31] and spermidine conjugates bearing large substituents on the secondary amino group have been found to be good transporter substrates.[26,32]

Cellular uptake of the synthesized complexes was quantitated for incubations with murine melanoma (B16) and Morris hepatoma (MH3924A) cells in culture and, for comparison, in a limited number of experiments with normal human hepatocytes and melanocytes. Furthermore, biodistribution and MRI studies were performed with rats bearing solid MH3924A tumors.

Results

Ligand Synthesis. The bis(amide) ligands **1**−**6** (Chart 1) were obtained by straightforward aminolysis reactions of DTPA-dianhydride with one (symmetric adducts) or two (asymmetric adducts) of the selected amine compounds listed in the Introduction. Boc protection of primary amino groups[33] was applied where necessary. After deprotection the ligands were complexed with Gd^{3+}, and the complexes **Gd-1** to **Gd-6** were purified by HPLC or obtained pure as precipitates from the reaction mixture.

Intracellular Uptake of Gadolinium Complexes. B16 melanoma and MH3924A hepatoma cells were incubated for 24 h in the presence of the gadolinium complexes with the synthesized ligands shown in Chart 1, using concentrations in the range 0−10 μM. For comparison, incubations with the unsubstituted Gd(DTPA) complex were performed. Following cell harvest and acid hydrolysis, inductively coupled plasma mass spectrometry (ICP−MS) with direct detection of gadolinium was used to quantitate uptake of complexes. For comparison, a few experiments were performed with normal human melanocytes and hepatocytes. The results are summarized in Figure 1. In the following, uptake values cited in the text refer to 10 μM incubations.

The uptake of $[Gd(DTPA)(H_2O)]^{2-}$ into B16 cells was below the ICP−MS detection limit (<0.0002 fmol/cell for instrument 1, see Methods). The uptake of **Gd-1** was concentration dependent (Figure 1A) and reached a maximum of 0.033 fmol/cell in B16 and 0.020 fmol/cell in MH3924A for the 10 μM incubation. For **Gd-2**, lacking the benzamide functional group, cellular uptake was a factor of 4−5 lower and appeared to plateau at ca. 0.006 fmol/cell (Figure 1A). Replacement of one 2-(diethylamino)ethylamide group (ligand **2**) with a bis(2-aminoethyl)amide moiety (ligand **3**) resulted in a dramatic increase in uptake for **Gd-3** vs **Gd-2**. This increase was a factor of 11 for B16 (0.083 fmol/cell) and 32 for the hepatoma cells (0.176 fmol/cell, Figure 1B). In contrast, the introduction of one lipophilic nonylamide function (ligand **4**) resulted in reduced uptake of **Gd-4** vs **Gd-2** by about a factor of 3 for B16 (0.0019 fmol/cell at 10 μM) and more than a factor of 10 for hepatoma (0.0004 fmol/cell). With the addition of a second bis(2-aminoethyl)amide substituent in **Gd-5**, uptake (0.030 fmol/cell in B16, 0.053 fmol/cell in MH3924A) was actually reduced by about a factor of 3 compared to **Gd-3** but was still higher than for **Gd-2**. Finally, **Gd-6**, which features two spermidine substituents, exhibited uptake that was similar to that of **Gd-3** at low incubation concentrations but somewhat lower for 10 μM incubations (0.063 fmol/cell for B16 and 0.108 fmol/cell for MH3924A), i.e., **Gd-6** uptake was intermediate between that of **Gd-3** and **Gd-5**. Thus, the polyamine-substituted complexes **Gd-3**, **Gd-5**, and **Gd-6** (Figure 1B) showed uniformly higher uptake in Morris hepatoma compared to B16 melanoma cells.

For comparison, a few experiments were performed with normal human hepatocytes and melanocytes in culture (Figure 1C). **Gd-6** showed higher uptake compared to **Gd-5** in hepatocytes (0.59 vs 0.15 fmol/cell), and in both cases the uptake was a factor 3−6 *higher* than in Morris hepatoma. The uptake of **Gd-6** into human melanocytes (0.026 fmol/cell) was a factor 2.4 *lower* than in B16 melanoma.

The data in Figure 1, expressed as fmol/cell, represent the actual measured amounts of gadolinium detected in harvested cells. The mean diameter of Morris hepatoma cells was estimated via light microscopy to be 15 ± 1 μm, yielding a mean cell volume of ca. 1.77 pL. Therefore, a gadolinium content of 1 fmol/cell corresponds to a concentration of ca. 570 μM. The uptake achieved for **Gd-3**, **Gd-5**, and **Gd-6** after 24 h for 10 μM incubations (Figure 1B) corresponds to intracellular concentrations in the range 20−100 μM. The resulting intra-to-extracellular concentration ratio (up to a factor 10) provides evidence for an active transport process.

Temperature Dependence of Intracellular Uptake. Figure 2A demonstrates that the uptake of **Gd-5** into MH3924A cells over 1 h was strongly reduced at 4 °C vs 37 °C. When cells

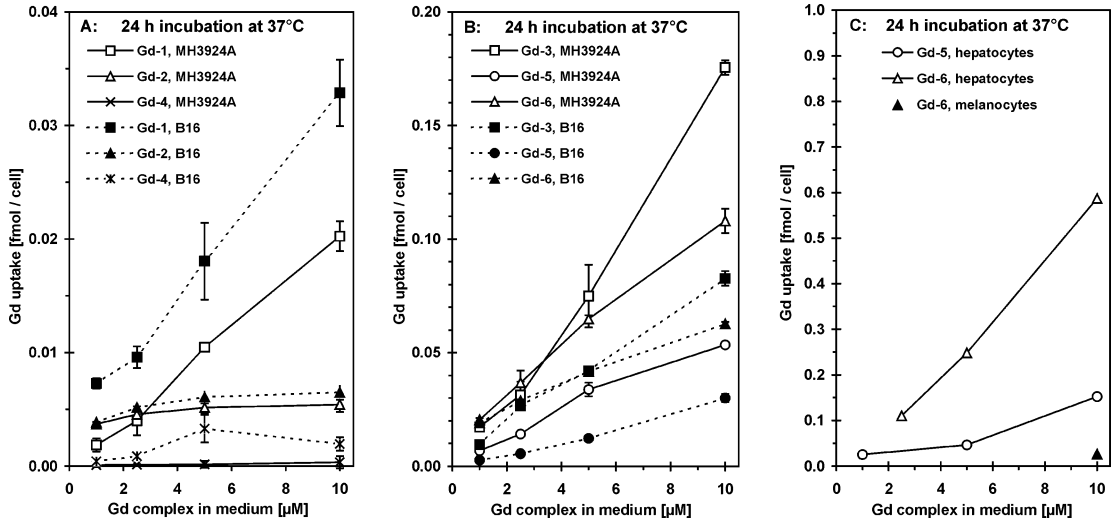

Figure 1. Intracellular uptake of gadolinium complexes into cultured cells after 24 h incubation at 37 °C, as determined by ICP−MS. (A) B16 melanoma or MH3924A Morris hepatoma with **Gd-1, Gd-2**, or **Gd-4**; $n = 1$ cell sample per determination; error bars denote SDs of replicate ICP−MS measurements with instrument 1. (B) B16 or MH3924A with **Gd-3**, **Gd-5**, or **Gd-6** ($n = 2$, instrument 2); error bars denote SDs for sample variance. Uptake of Gd(DTPA) into tumor cells was <0.001 fmol/cell and below the detection limit for our ICP−MS protocol. (C) Uptake of **Gd-5** or **Gd-6** into human hepatocytes or melanocytes at selected incubation concentrations ($n = 1$, measurement SD < 2%). Note: the vertical scales of the three graphs increase by a factor of 5 from A to B and from B to C. Uptake of 1 fmol/cell corresponds to ca. 570 μM intracellular concentration for tumor cells.

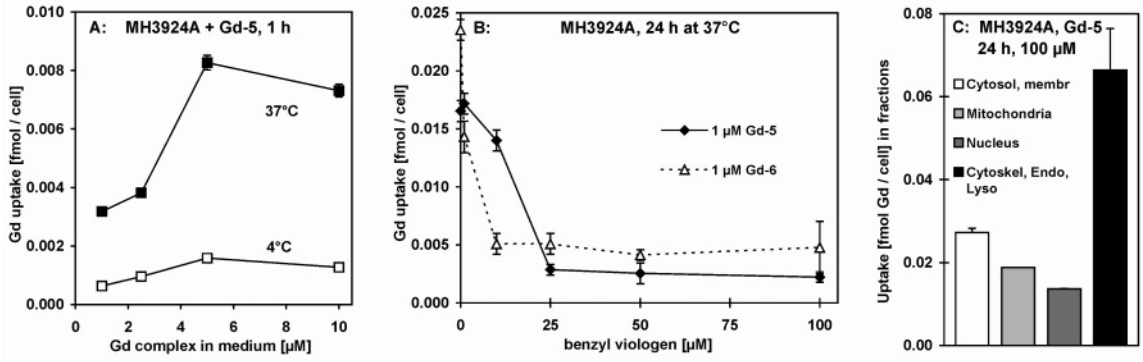

Figure 2. (A) **Gd-5** uptake into MH3924A cells after 1 h incubations at 4 °C and 37 °C ($n = 1$). (B) Inhibition assay for uptake of **Gd-5** or **Gd-6** into MH3924A cells (24 h incubations with 1 μM complex at 37 °C, $n = 2$) in the presence of the polyamine uptake inhibitor benzyl viologen. (C) Distribution of **Gd-5** in four subcellular fractions of MH3924A cells [(1) cytosol and plasma membranes, (2) mitochondria, (3) nucleus, (4) cytoskeleton, endosomes, and lysosomes] after 24 h incubation with 100 μM at 37 °C ($n = 1$ for mitochondria, otherwise $n = 2$).

that had been tested at 4 °C were subsequently incubated at 37 °C, uptake of **Gd-5** was restored to the levels observed with freshly harvested cells. The temperature dependence of passive diffusion alone is proportional to T/η, where η is the solvent viscosity at temperature T. This leads to the prediction that the uptake rate should decrease by at least a factor of 2.5 at 4 °C vs 37 °C. The observed decrease in uptake shown in Figure 2A was about a factor of 5−6.

Inhibition of Intracellular Uptake. An inhibition assay with the polyamine uptake inhibitor benzyl viologen is shown in Figure 2B. For incubations of MH3924A cells with 1 μM **Gd-5** or **Gd-6**, uptake of CA was effectively inhibited to plateau levels of 14% or 19%, respectively, for benzyl viologen concentrations greater than 25 μM. The estimated IC_{50} values were 16 and 1.3 μM with **Gd-5** and **Gd-6**, respectively.

Subcellular Distribution. Following a 24 h incubation of MH3924A with 100 μM **Gd-5** at 37 °C, the ProteoExtract kit was used to isolate four subcellular fractions: (1) cytosol and plasma membranes, (2) mitochondria, (3) nucleus, (4) cytoskeleton, endosomes and lysosomes. Under these conditions total uptake of contrast agent was 0.126 fmol/cell, and the distribution into fractions 1 to 4 was 22, 15, 11, and 52%, respectively (Figure 2C). Thus, the highest concentration of **Gd-5** was found in the cytoskeleton fraction.

Cellular Toxicity. Cellular toxicities of **Gd-3**, **Gd-5**, **Gd-6**, and Gd(DTPA) were tested in an MTS assay with MH3924A cells. Incubations with gadolinium complex at concentrations of 1−100 μM were performed for 48 h, and cell survival (percentage relative to untreated controls) ranged between 90% and 118%. There were no significant differences between different complexes or between complex and control (data not shown).

Serum Albumin Binding. Incubation of **Gd-3**, **Gd-5**, or **Gd-6** with human serum albumin for 30 or 90 min at 37 °C (see Methods) resulted in no significant binding of complex to protein, e.g., 93 ± 6% of **Gd-3** was found to be free. This situation was considered to be favorable for in vivo studies.

Biodistribution and Excretion Data. Individual ACI rats bearing a subcutaneous MH3924A tumor in the right thigh received an intravenous bolus injection of Gd(DTPA), **Gd-5**, or **Gd-6**. At 1 h or 24 h postinjection animals were sacrificed and the Gd content of various tissues, blood, and in some cases urine and faeces was determined by ICP−MS. The data are summarized in Table 1 and expressed as *concentrations* (nmol

Table 1. Biodistribution of Gd(DTPA), **Gd-5**, and **Gd-6** (Concentration in nmol/g) and Cumulative Excretion for Tumor-Bearing ACI Rats[a]

tissue	**Gd(DTPA)**, 1 h	**Gd-5**, 1h	**Gd-5**, 24 h	**Gd-6**, 1 h	**Gd-6**, 24 h
tumor (MH3924A)	3.1	5.5	0.6	7.2	0.8
liver	3.0	4.2	2.0	6.6	5.5
kidney (+urine)	40.7	120.3	40.9	141.6	62.3
lung	4.1	12.7	24.2	20.2	5.9
blood	4.8	7.8	0.1	4.8	0.1
muscle (femur)	1.3	1.6	n.a.	n.a.	n.a.
spleen	1.5	4.7	n.a.	n.a.	n.a.
bone (femur)	0.8	2.2	0.9	3.3	1.0
bone marrow (femur)	1.5	0.8	1.7	0.9	2.3
small intestine	1.8	18.9	0.4	4.0	0.1
brain	0.4	0.5	n.a.	n.a.	n.a.
urine (cumulative)	25805	2116	537	n.a.	650
faeces	n.a.	n.a.	16.6	n.a.	41.4
excretion % of total dose	n.a.	n.a.	98	n.a.	94

[a] Rats were sacrificed 1 h or 24 h postinjection of contrast agent; tissues and biofluid samples were hydrolyzed and analyzed by ICP−MS to give Gd concentration in nmol/g tissue or fluid. Each column of data represents results for one animal, scaled proportionally to correspond to a constant Gd dose of 100 μmol/kg body wt.; n.a. = sample not available. After 24 h Gd(DTPA) was below the ICP−MS detection limit (ca. 0.03 nmol/g) for tumor, liver, or kidney.

per g tissue or fluid) after linear scaling to correspond to a constant dosage of 100 μmol/kg, as typically used for MRI (see Methods). In general, at 1 h postinjection **Gd-5** and **Gd-6** exhibited higher tissue concentrations and lower urine concentrations compared to Gd(DTPA), in particular for tumor, liver, kidney (uncorrected for urine content), lung, and small intestine. At 24 h postinjection Gd(DTPA) could not be detected in tumor, liver, or kidney by our ICP−MS protocol (<0.03 nmol/g) while the polyamine-substituted agents were still present in significant amounts. The cumulative excretion of **Gd-5** and **Gd-6** in urine and faeces was calculated to be, respectively, 98% and 94% of total dose.

Relaxivities of Gd-DTPA-Polyamine Complexes. MRI techniques were used to simultaneously measure the longitudinal relaxation rates $R_1 = 1/T_1$ for water protons in the following reference solutions at 300.13 MHz and 25 °C: (1) phosphate-buffered saline (PBS) at pH 7.4; (2,3,4) 1 mM **Gd-3**, **Gd-5**, or **Gd-6** in PBS. The R_1 values summarized in Table 2 have standard errors of estimate (SE) of <0.1%, and the calculated relaxivities r_1 for **Gd-3**, **Gd-5**, and **Gd-6** are 6.23, 5.59, and 6.86 s^{-1} mM^{-1}, respectively. For comparison, R_1 for a 5 mM solution of Gd(DTPA) in PBS was measured under identical conditions using a spectroscopic inversion−recovery method. The calculated r_1 of 3.81 s^{-1} mM^{-1} agrees well with literature values of 3.00 ± 0.56 (6.3 T, 37 °C) for Gd(DTPA) in aqueous solution[34] and $r_1 = 4.02 \pm 0.14$ (4.7 T, room temperature) or 3.87 ± 0.06 (8.45 T, room temperature) for Gd(DTPA) in saline.[35]

Intracellular Relaxivities. Cultured MH3924A tumor cells were incubated at 37 °C for 24 h with the selected CA (**Gd-3**, **Gd-5**, or **Gd-6**) at 0, 10, 30, or 75 μM. Relaxation rates R_1 at 300.13 MHz and 25 °C for harvested cell pellets in glass capillaries were determined by MRI as described above and in the Experimental Section. For each incubation an aliquot of 1.5×10^6 cells was frozen for later determination of the intracellular Gd concentration by ICP−MS. The measured Gd concentrations and the observed relaxation rates R_{1obs} are summarized in Table 2 ($n = 1$ determination for each incubation). Monoexponential relaxation behavior was observed, consistent with fast exchange of water between the intra- and extracellular compartments. Therefore, for a simple two-site model, R_{1obs} represents the weighted average of the intra- and extracellular relaxation rates R_{1in} and R_{1ex}. The mole fraction for intracellular water $f_{in} = 0.32$ was determined by Terreno et al.[36] for rat hepatocarcinoma cell pellets, and, in the absence of specific data for our cell pellets, this value was used to calculate the intracellular relaxation rates R_{1in} listed in Table 2 (via eq 1). Finally, the molar relaxivities r_{1obs} (for the cell pellet as a whole) and r_{1in} (for a hypothetical homogeneous intracellular compartment) were calculated from the relaxation rates and the intracellular Gd concentrations determined by ICP−MS (Table 2, see Experimental Section).

In the relaxivity study the incubations performed with 10 μM CA correspond to the highest concentration used for the experiments of Figure 1B. The intracellular concentrations of Gd complex obtained, namely, 0.151 fmol/cell (86 μM) for **Gd-3**, 0.071 fmol/cell (40 μM) for **Gd-5**, and 0.113 fmol/cell (64 μM) for **Gd-6**, are comparable to the mean values shown in Figure 1B. For the relaxation measurements higher incubation concentrations were also tested. At 30 μM CA there was a less than proportional increase in CA uptake, and no further increase was observed for the 75 μM incubations. Thus, CA uptake over 24 h is either saturated at extracellular concentrations of 30 μM, or an equilibrium is reached between import and export of CA. The range of intracellular Gd concentrations in Table 2 corresponds to $(0.43-1.42) \times 10^8$ atoms per cell.

The relaxation data show that for MH3924A cells without CA, $R^0_{1obs} = 0.44-0.48$ s^{-1}. Assuming $R^0_{1ex} = 0.337$ s^{-1} (PBS), we obtain $R^0_{1in} = 0.67-0.78$ s^{-1}. For **Gd-3** and **Gd-6** with intracellular concentrations ranging from 64 to 133 μM, $R_{1obs} = 1.10-1.33$ s^{-1} (SE < 1%), which translates to $r_{1obs} = 6.0-10.3$ and $r_{1in} = 19-32$ s^{-1} mM^{-1}. For **Gd-5** with lower intracellular concentrations (40−61 μM) somewhat higher relaxation rates were observed (1.35−1.45 s^{-1}, SE < 3%), implying $r_{1obs} = 14.2-23.5$ and $r_{1in} = 45-73$ s^{-1} mM^{-1}.

Magnetic Resonance Imaging in Vivo. A pilot series of MRI experiments with ACI rats bearing a subcutaneous MH3924A tumor in the right thigh was performed at 2.35 T, as described in the Experimental Section. The anesthetized animals received an intravenous bolus injection (100 μmol/kg) of Gd(DTPA), Gd(DO3A-butrol)) or one of the polyamine-substituted complexes **Gd-3**, **Gd-5**, or **Gd-6**. Multislice transverse and coronal images were obtained 1 h post Gd with either T_1- or T_2-weighting and after 24 h with T_1-weighting. Individual transverse slices covering the central tumor region are compared in Figure 3.

With T_2 weighting the tumor was delineated as a hyperintense area, independent of contrast agent, with a contrast ratio of 2.0−2.3 relative to neighboring muscle tissue. With T_1 weighting at 1 h post Gd, there was low contrast for tumor vs muscle tissue with Gd(DO3A-butrol) (maximum contrast ratio = 1.06; similar results for Gd(DTPA), not shown) while accumulation of the polyamine complexes could be visualized as regional hyperintensity in the tumor with contrast ratios of 1.22, 1.11, and 1.49 for **Gd-3**, **Gd-5**, and **Gd-6**, respectively. At this time point all contrast agents showed high accumulation in the kidneys and urine-filled bladder. Even after 24 h sufficient concentrations of polyamine complex were still present in tumor, resulting in regional hyperintensity with contrast ratios of 1.11, 1.08, and 1.21 for **Gd-3**, **Gd-5**, and **Gd-6**, respectively. With Gd(DTPA) hyperintensity in tumor could be detected at 10−15 min post Gd and also at 1 h when a 3.6-fold higher dose was used (data not shown), but in all cases at 24 h the extracellular agent was cleared from tumor, and no contrast with T_1 weighting was achieved.

Table 2. Relaxivities of Gd-DTPA-Polyamines in Solution and in Cultured MH3924A Cells

		intracell. Gd (ICP−MS)		relax. rates[a] (3-param. fit)			relaxivity[b]	
sample[c]	24 h incub.[d] (μM CA)	(fmol/cell)	(mM)	R_{1obs} (s^{-1})	SE (s^{-1})	calcd[e] R_{1in} (s^{-1})	r_{1obs} (s^{-1} mM^{-1})	r_{1in} (s^{-1} mM^{-1})
PBS, pH 7.4				0.3368	0.0006			
1 mM **Gd-3**				6.571	0.018		6.23	
1 mM **Gd-5**				5.926	0.025		5.59	
1 mM **Gd-6**				7.196	0.025		6.86	
5 mM Gd(DTPA)				19.39	0.048		3.81	
MH + **Gd-3**	0	<0.0002	0	0.449	0.002	0.69		
	10	0.151	0.086	1.109	0.006	2.75	7.71	24.1
	30	0.231	0.130	1.224	0.011	3.11	5.95	18.6
	75	0.236	0.133	1.328	0.010	3.43	6.60	20.6
MH + **Gd-5**	0		0	0.478	0.006	0.78		
	10	0.071	0.040	1.423	0.039	3.73	23.5	73.4
	30	0.108	0.061	1.349	0.035	3.50	14.2	44.5
	75	0.106	0.060	1.448	0.041	3.81	16.3	50.8
MH + **Gd-6**	0		0	0.444	0.001	0.67		
	10	0.113	0.064	1.103	0.005	2.73	10.3	32.3
	30	0.179	0.101	1.229	0.006	3.13	7.78	24.3
	75	0.179	0.101	1.258	0.006	3.22	8.03	25.1

[a] Water proton relaxation rates for the polyamine derivatives were determined by 2D saturation−recovery spin−echo MRI with slice-selective 180° pulse and 16 recovery times; for Gd(DTPA) by spectroscopic inversion−recovery with 12 recovery times; mean ROI intensities or signal integral (Gd(DTPA)) were fitted with a three-parameter monoexponential function; SE = standard error of estimate for fitted parameters. [b] Molar relaxivity r_{1obs} calculated from R_{1obs}; intracellular r_{1in} calculated from R_{1in}. [c] All reference solutions and cell pellets in PBS, pH 7.4. [d] Standard culture conditions for MH cells with CA added for 24 h, 37 °C. Only one control cell sample with 0 μM CA was prepared; it was measured three successive times together with each set of samples for a given CA. [e] R_{1in} for intracellular water calculated from R_{1obs} assuming two-site fast exchange with intracellular fraction $f_{in} = 0.32$ and $R_{1ex} = R_{1obs}$ for PBS.

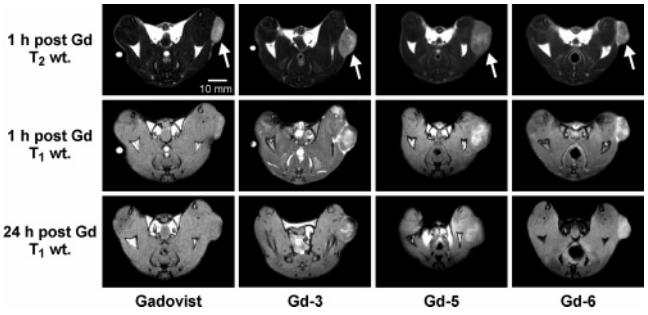

Figure 3. Transaxial MR images (2.35 T) were obtained with T_2 weighting (spin echo with TR/TE = 2000/32 ms) or T_1 weighting (gradient echo with TR/TE = 212/5 ms, 60° flip angle) from four anesthetized ACI rats, each bearing a subcutaneous MH3924A tumor in the right thigh (arrow). The images (2 mm slices, 0.55 mm pixel resolution) from each individual animal (vertical column) were obtained at 1 h or 24 h post intravenous injection of 100 μmol/kg of the indicated contrast agent. Regional T_1-weighted contrast enhancement in the partially necrotic tumors is observed at 24 h only with the polyamine-substituted agents **Gd-3**, **Gd-5**, or **Gd-6**. Gd(DTPA) gave results similar to those of Gd(DO3A-butrol).

At 1 h post Gd the T_2-weighted images shown in Figure 3 (TE = 32 ms) exhibit moderate intensity variations within tumor that show the same pattern in the images at TE = 8 ms and are, therefore, mainly due to spin density variations. For the polyamine contrast agents the images at TE = 96 ms show hypointense regions (shortest T_2) which coincide with the hyperintense regions (shortest T_1) in the displayed T_1-weighted images. In general, the tumors exhibited heterogeneous uptake of polyamine contrast agent, with large signal intensity variations within and between the individual image slices. For **Gd-3** or **Gd-6** in Figure 3, the tumor periphery and internal regions showed hyperintensity with T_1 weighting at 1 h post Gd.

Discussion

Uptake and Distribution. In this study we have demonstrated that the extracellular MR contrast agent Gd(DTPA) can be transformed into a membrane-permeable, intracellular agent by the addition of two positively charged functional groups such as procainamide or 2-(diethylamino)ethylamine to the DTPA ligand. Thus, the intracellular uptake of **Gd-1** into B16 or MH3924A tumor cells reached concentrations on the order of 10−20 μM (1 fmol/cell = ca. 570 μM) after 24 h incubations with 10 μM contrast agent (Figure 1A). Cellular uptake was improved, leading to intracellular concentrations in the range of 20−100 μM, when the polyamine bis(2-aminoethyl)amine or spermidine was employed as DTPA substituent (Figure 1B), with **Gd-3** and **Gd-6** giving the best results. The subcellular distribution in hepatoma cells was determined for **Gd-5** only (Figure 2C) and indicated that there was a clear preference of CA for fraction 4, which contains elements of the cytoskeleton to which endosomes and lysosomes are bound,[37] i.e., compartments where polyamines are known to be localized.[31]

Preliminary experiments (Figure 1C) demonstrated a substantially higher uptake of **Gd-6** into normal human hepatocytes compared to melanocytes, and higher uptake efficiency for **Gd-6** vs **Gd-5** into hepatocytes was confirmed, analogous to the results for Morris hepatoma. The in vivo biodistribution results (Table 1) indicated that **Gd-5** and **Gd-6** accumulated not only in hepatoma but also to similar or higher concentrations in liver, lung, small intestine, and kidney in particular. However, for kidney (not flushed) a substantial contribution to the CA content from fresh urine is likely and is reflected in the high content of Gd(DTPA) also found in the kidney at 1 h postinjection. At 24 h Gd(DTPA) could not be detected in tumor, liver or kidney, indicating that the urine contribution at this time was negligible. Thus, the high concentrations of **Gd-5** and **Gd-6** still present in kidney after 24 h represent tissue (intracellular) uptake. The distribution pattern observed for these agents after 24 h closely resembles the pattern observed in mice by Zhuo et al.[38] after 4-day treatment with a polyamine-based boron complex designed for neutron-capture therapy (relative concentrations: kidney > liver > B16 melanoma > muscle). Thus, the tissue distribution of our polyamine-substituted Gd(DTPA) complexes appears to follow the basic pattern known for the endogenous polyamines and lends support to our hypothesis that intracellular

uptake of these complexes is facilitated by polyamine transporters. Note that the substantial concentration of Gd(DTPA) detected in tumor *tissue* is not in conflict with the absence of uptake in cultured tumor *cells* but in fact reflects the contributions of the vascular and interstitial compartments for this extracellular agent in vivo.

Tumor Specificity and the Role of Polyamine Transporters. Our original goal of developing gadolinium complexes with high melanoma affinity by introducing melanin-binding pharmacophores into the side chains of DTPA was realized to some extent with **Gd-1** but not with **Gd-2**. The higher accumulation of **Gd-1** in B16 vs MH3924A cells presumably involves melanosome binding and can be attributed to the 2-(diethylamino)ethylamine terminal substituents. Analogous behavior was observed with technetium complexes containing similar structural elements.[17−19] The better performance of **Gd-1** vs **Gd-2** implicates the importance of the benzamide moiety as well. The replacement of one melanin-binding pharmacophore with a polyamine substituent to give **Gd-3** resulted in a remarkable increase in uptake for both tumor cell lines due to increased affinity for the polyamine transporter. All three polyamine-substituted DTPA complexes exhibited higher affinity for Morris hepatoma cells vs B16 melanoma, consistent with the expected higher expression of polyamine transporters in hepatoma (hepatocytes) vs melanoma (melanocytes).

More convincing support for the role of polyamine transporters in the uptake of **Gd-5** and **Gd-6** is provided by the inhibition experiment shown in Figure 2B. The known transporter inhibitor benzyl viologen reduced the uptake of our complexes to a plateau level of ca. 15%. This residual uptake occurs apparently via other mechanisms not requiring polyamine transporters.

Thus, we have sufficient evidence that the new class of Gd-DTPA-polyamine contrast agents, represented by the complexes **Gd-3**, **Gd-5**, and **Gd-6** can be efficiently imported via polyamine transporters, which are typically upregulated in highly proliferating or malignant cells such as the MH3924A and B16 lines chosen for this study.[26,29] However, uptake is also expected to be high in those normal tissues such as liver and kidney which also have high polyamine storage or turnover.

Complex Stability. Cabella et al.[39] have shown that rat hepatoma (HTC) and rat glioma (C6) cells incubated with 1.6 mM Gd-DTPA-BMA, the bis(methylamide) derivative of Gd(DTPA), exhibit a ca. 10-fold higher binding + uptake of Gd (ca. 10 fmol/cell), compared to Gd(HPDO3A), Gd(DOTA), and Gd(DTPA). This behavior was explained as a "sponge" effect. Since the thermodynamic stability constant of Gd-DTPA-BMA is significantly lower (6−8 orders of magnitude) than for the other complexes, chelator stripping at the cell membrane surface results in internalization of Gd as ca. 98% uncomplexed Gd^{3+}. Such uptake is not saturable, and the resulting intracellular Gd^{3+} causes a loss of cell viability. Therefore, Cabella et al.[39] have warned against the use of bisamide Gd-DTPA derivatives in the development of new CAs.

We have no evidence that such a Gd internalization mechanism is operating for the Gd-DTPA-polyamine derivatives described here. Cellular uptake exhibits saturation effects at incubation concentrations above 30 μM and is strongly reduced by an inhibitor of polyamine transport. No effect on cell viability was observed at 100 μM incubations. Finally, the more stable Gd-DOTA-polyamine derivatives that we have examined in preliminary experiments show similar or higher cellular uptake in comparison with the Gd-DTPA-polyamines.

Relaxivity. The data summarized in Table 2 show that the three Gd-DTPA-polyamines in solution have similar relaxivities in the range 5.6−6.9 s^{-1} mM^{-1} at 300 MHz and 25 °C. These values are somewhat higher than the value of 3.8 s^{-1} mM^{-1} determined for Gd(DTPA) under identical conditions or r_1 values of ca. 3.5−5 measured at 20 MHz for many of the common agents with DTPA, DOTA, or DO3A ligands.[1] The data of Table 2 also show that **Gd-5** produces relaxation enhancement in cultured cell pellets similar to that observed for **Gd-3** and **Gd-6**, even though the intracellular concentration of **Gd-5** is about a factor of 2 lower. Thus, in cultured cells the molar relaxivities for **Gd-5** are correspondingly higher.

The parameter r_{1obs} in Table 2 represents (a) an effective relaxivity for the entire cell pellet, independent of the (unknown) details of CA compartmentation, and (b) a lower limit for the intracellular $r_{1in,}$ which can be estimated using a simple two-compartment model with fast exchange of water across the cell membrane and with CA distributed in a (homogeneous) intracellular water fraction with $f_{in} = 0.32$, as determined by Terreno et al.[36] The fast-exchange condition appears to be justified by the monoexponential relaxation observed, the low concentrations of CA involved ($\ll 2 \times 10^9$ molecules/cell) and relaxation enhancements that are much lower than the water exchange rate.[36] The two-site analysis leads to rather high intracellular relaxivities, suggesting that the contrast agent is involved in binding equilibria with macromolecules or subcellular structures. Actually, we know from the cellular distribution experiments (Figure 2C) that a major fraction of intracellular **Gd-5** is associated with the subcellular fraction 4 which includes the cytoskeleton, endosomes and lysosomes—elements where polyamines tend to accumulate. We do not have data for the distribution of the other complexes, but the relaxivity results suggest that **Gd-3** and **Gd-6** may have less affinity for macromolecular structures.

For **Gd-3**, **Gd-5**, and **Gd-6** the highest relaxivities were obtained with the 10 μM incubations (r_{1obs} = 7.7, 23.5, 10.4, respectively), while somewhat lower values were obtained for the 30 μM and 75 μM incubations (mean r_{1obs} = ca. 6.3, 15.2, 7.9), where higher intracellular CA concentrations were achieved. Such a reduction of relaxivity (quenching) with increasing CA concentration has been described by Terreno et al.[36] and others.[14,40] The effect can be explained by the sequestering of CA in a compartment with a small volume fraction, e.g., in endosomes due to uptake via pinocytosis, where the resulting high local relaxation rate in comparison to a slower exchange rate (slow-exchange condition) essentially decouples this compartment from the cytosol compartment. Therefore, the observable relaxation enhancement saturates with increasing CA concentration, and relaxivity decreases. Such an effect may be operating for our polyamine-substituted CAs, since Figure 2C indicates that a substantial fraction of the CA is taken up into organelles such as endosomes, mitochondria, and the nucleus.

Contrast Enhancement in Vivo. The Gd-DTPA-polyamine complexes proved to be nontoxic for cultured MH3924A cells at concentrations up to 100 μM, exhibited favorable relaxivity characteristics, and were considered safe for initial imaging experiments. MRI contrast enhancement at bolus doses of 100 μmol/kg was expected for tumor vs muscle, for example, and was confirmed by the results in Figure 3. The retention of detectable levels of the polyamine contrast agents in Morris hepatoma even after 24 h was demonstrated by MRI and the biodistribution data, and such performance could not be achieved with conventional extracellular agents such as Gd(DTPA) or Gd(DO3A-butrol). The in vivo results indicate that the three CAs tested are approximately equivalent in their contrast enhancement behavior, in agreement with the roughly equal

relaxation enhancements (R_{1obs} in Table 2) observed for cultured hepatoma cells, despite the significantly lower uptake of **Gd-5**. Although the three polyamine-substituted DTPA complexes exhibited somewhat higher affinity for the Morris hepatoma cells, uptake into B16 melanoma cells was also substantial (Figure 1B) and should be sufficient for contrast enhancement in MRI applications.

Summary. This study illustrates the potential of utilizing polyamine transporters for facilitated uptake of MRI contrast agents into tumors in general. The Gd-DTPA-polyamine complexes tested exhibited suitable relaxivities in solution, high intracellular relaxivities, and high T_1-weighted contrast for s.c. tumors vs muscle. However, the detection of tumors within organs with naturally high polyamine uptake may prove to be difficult. Work is in progress with alternative chelators such as DOTA, and additional studies with other tumor types and host tissues are needed. We hope that this research will stimulate the development of new and clinically applicable intracellular MRI imaging agents for tumor diagnosis.

Experimental Section

General Information. All chemicals were purchased from Sigma-Aldrich (Taufkirchen, Germany). Spectroscopic analysis for structure confirmation was performed by electrospray mass spectrometry (ESI-MS, Finnigan TSQ 7000; Thermo Electron Corp, Bremen, Germany) and 250 MHz NMR spectroscopy (AC-250; Bruker BioSpin GmbH, Rheinstetten, Germany). In general, ligand purifications were accomplished by preparative HPLC with a Lichrosorb 60 RP Select B column (250 × 10 mm, 10 μm; Merck KGaA, Darmstadt, Germany) with an eluent flow rate of 3.7 mL/min and ultraviolet detection at 206 nm (SPD-10A VP; Shimadzu, Duisburg, Germany). The eluent comprised 0.1% trifluoroacetic acid (TFA) in water (solvent A) and 0.1% TFA in acetonitrile (solvent B) with a linear gradient of 0% to 100% B in A applied over 30 min. The purity of ligands and Gd complexes was confirmed by two different analytical HPLC procedures, the details of which are summarized along with the spectroscopic data for the synthesized compounds (NMR, MS) in the Supporting Information.

Chemistry. DTPA Bisamide of Procainamide (1). A mixture of DTPA-dianhydride (357 mg, 1 mmol) and procainamide (544 mg, 2 mmol) was stirred in anhydrous DMF for 24 h. Solvent evaporation under reduced pressure gave an oily residue which was purified by preparative HPLC to give 109 mg of **1** (yield: 13.2%).

DTPA Bisamide of 2-(Diethylamino)ethylamine (2). A mixture of DTPA-dianhydride (357 mg, 1 mmol) and 2-(diethylamino)-ethylamine (232 mg, 2 mmol) was stirred in anhydrous DMF for 24 h. Solvent evaporation under reduced pressure gave an oily residue which was purified by preparative TLC on silica, using CH_3OH/Et_3N (95/5) as the eluent and ninhydrin as detection reagent, yielding 78 mg of **2** (yield: 13.2%).

Mixed DTPA Amide of 2-(Diethylamino)ethylamine and Bis-(2-aminoethyl)amine (3). The primary amino groups of bis(2-aminoethyl)amine (2.5 g, 8.25 mmol) were Boc protected (Boc = *t*-butyloxycarbonyl) using a method of Rannard and Davis[33] to give 1.58 g of N^1,N^3-bis(*t*-butyloxycarbonyl)-bis(2-aminoethyl)amine (yield: 63%). A mixture of this Boc-protected amine (303 mg, 1 mmol) and 2-(diethylamino)ethylamine (116 mg, 1 mmol) was reacted with DTPA-dianhydride (714 mg, 2 mmol) in anhydrous DMF for 24 h. Purification was accomplished by preparative HPLC. The product-containing fractions were lyophilized to give 37 mg of Boc_2-protected **3** (yield: 4.8%). Deprotection was performed at ambient temperature for 24 h with a mixture of trifluoroacetic acid, water, and triisopropylsilane (90/9/1). Precipitation from methanolic solution with diethylether resulted in 25 mg of **3** (yield: 4.3%).

Mixed DTPA Amide of 2-(Diethylamino)ethylamine and Nonylamine (4). DTPA-dianhydride (2 mmol) was reacted with a mixture of 2-(diethylamino)ethylamine (116 mg, 1 mmol) and nonylamine (143 mg, 1 mmol) as above. Workup was performed as described for ligand **2** to give 54 mg of **4** (yield: 8.8%).

DTPA Bisamide of Bis(2-aminoethyl)amine (5). Two equivalents of N^1,N^3-bis(Boc)-bis(2-aminoethyl)amine (606 mg, 2 mmol) were reacted with DTPA-dianhydride (1 mmol) as above. Purification of the Boc_4-protected product was accomplished by preparative HPLC. Deprotection and workup was performed as described for ligand **3** to give 104 mg of **5** (yield: 18.4%).

DTPA Bisamide of Spermidine (6). The primary amino groups of spermidine were selectively protected according to Rannard and Davis[33] to give N^1,N^3-bis(Boc)-spermidine, two equivalents of which (700 mg, 2 mmol) were reacted with DTPA-dianhydride (357 mg, 1 mmol) as above. The Boc_4-protected product was purified by preparative HPLC. Deprotection was performed as for ligand **3** to give 85 mg of **6** (yield: 13%).

Gadolinium Complexes. The complexes **Gd-1** to **Gd-6** were formed at 90 °C in aqueous solution using gadolinium(III)acetate and equimolar amounts of the corresponding ligands **1** to **6**. Complex **Gd-1** was purified by preparative reverse-phase HPLC. Complexes **Gd-2** to **Gd-6** were obtained from the reaction mixture by solvent evaporation and subsequent crystallization from MeOH and diethylether as white solids. The commercial agents Gd(DTPA) and Gd(DO3A-butrol) were obtained from Schering (Berlin, Germany).

Cell Culture. B16 melanoma cells (mouse) and MH3924A Morris hepatoma cells (rat) were obtained from the German Cancer Research Center (DKFZ) tumor bank and grown at 37 °C as stock cultures in RPMI 1640 supplemented with 10% fetal calf serum and 1% glutamine as standard medium under a 5% CO_2 atmosphere (all components: Pan Biotech GmbH, Aidenbach, Germany). For contrast agent uptake studies 10^6 cells were inoculated into 25 cm^2 culture flasks (BD Biosciences, Bedford, USA) and grown for 24 h in 10 mL of the standard culture medium. Cells were then incubated for an additional 24 h (1 h for temperature dependence studies) with fresh medium containing 0, 1, 2.5, 5, or 10 μM of the selected gadolinium complex. Afterward the medium was removed, cells were trypsinated, washed twice, resuspended in culture medium, and counted. Aliquots containing 2.5, 3.0, or 3.5 million cells in 100 μL of PBS were submitted for Gd analysis by ICP−MS (n = 1 sample per incubation for **Gd-1**, **Gd-2**, and **Gd-4**; n = 2 for **Gd-3**, **Gd-5**, and **Gd-6**) as described below.

For comparison with the results for B16, 250 000 human melanocytes (Promo Cell, Heidelberg, Germany) were incubated for 24 h with 0 or 10 μM **Gd-6** in melanocyte growth medium (Promo Cell). Cells were harvested as above and submitted for ICP−MS (n = 1).

Cultured human hepatocytes (Cytonet GmbH, Weinheim, Germany) embedded in a collagen matrix in a 12-well microtiter plate (600 000 viable cells per well) were incubated for 24 h in hepatocyte growth medium (Cytonet) with various concentrations of **Gd-5** or **Gd-6**. Control incubations were performed under identical conditions with equal portions of cell-free collagen matrix to account for the substantial binding of contrast agent to the matrix alone. After incubation the medium was removed, wells were washed twice with PBS, and cells + matrix were dissolved with nitric acid and transferred completely to an Eppendorf vial for the subsequent extraction steps and ICP−MS (n = 1). Results are reported for cell + matrix samples minus collagen controls.

Polyamine Transport Inhibition. Aliquots of 10^6 MH3924A cells were inoculated into 25 cm^2 culture flasks and grown for 24 h in 10 mL of the standard culture medium. Cells were then incubated for an additional 24 h with fresh medium containing 1 μM of **Gd-5** or **Gd-6** and 0, 1, 10, 25, 50, or 100 μM of the polyamine uptake inhibitor benzyl viologen.[41,42] Cells were harvested as above and gadolinium content was determined by ICP−MS (n = 2).

Subcellular Distribution. Aliquots of 5×10^6 MH3924A cells were grown in 25 cm^2 culture flasks as above and incubated for 24 h with 100 μM **Gd-5**. The Subcellular Proteome Extraction Kit ProteoExtract (Merck, Darmstadt, Germany) was used according to the instructions of the manufacturer to isolate four cellular fractions: (1) cytosol and plasma membranes, (2) mitochondria, (3) nucleus, (4) cytoskeleton, endosomes, and lysosomes.

The gadolinium content for each fraction was determined by ICP−MS ($n = 2$ samples for fractions 1, 3, and 4; $n = 1$ sample for fraction 2).

Cytotoxicity Studies. B16 or MH3924A cells were cultured for 24 h in a 96-well plate under our standard conditions and then incubated for 48 h with fresh medium containing the chosen CA at various concentrations from 0 to 100 μM. The number of surviving cells was measured by the MTS viability assay (Cell Titer 96 Aq_{ueous}; Promega, Madison, WI). Formazan dye formation was determined by optical absorption at 490 nm with a microplate reader (model 3350-UV, Biorad Laboratories GmbH, Munich, Germany). Cell survival was expressed as percent of controls for $n = 4$ determinations.

Serum Albumin Binding. Solutions containing 20 μM **Gd-3**, **Gd-5,** or **Gd-6** and 40 g/L human serum albumin (Behring, Bern, Switzerland) were incubated at 37 °C for 30 or 90 min. The solutions were subjected to ultrafiltration (filter cutoff 20 kD; Sartorius, Göttingen, Germany), and the amount of unbound complex in the ultrafiltrate was determined with ICP−MS ($n = 2$).

Animal Models. For in vivo tumor studies 2×10^6 MH3924A tumor cells were injected subcutaneously into the right thigh of male ACI rats (Charles River, Sulzfeld, Germany) weighing 220−260 g. All animal experiments were performed in compliance with the German Animal Protection Laws (Permit 35-9185.81/G-7-03, Reg.-Praesidium, Karlsruhe, Germany).

Biodistribution and Excretion Data. At 14 days after inoculation (tumor diameter 5−6 mm), each animal was given an i.v. injection (tail) of the chosen CA (Gd(DTPA), **Gd-5**, or **Gd-6**; dose range 50−300 μmol/kg) and placed in a metabolic cage for the collection of urine and faeces. At 1 h or 24 h postinjection the animals were weighed, sacrificed by cervical dislocation, and dissected. Blood (ca. 6 mL) was extracted from the aorta with a syringe. Organs or tissues were blotted dry and weighed. For the 1 h experiments urine was extracted from the bladder via syringe, when possible. Samples containing a maximum of 500 mg of individual tissues were homogenized in glass tubes, digested with 1 mL of 50% concentrated HNO_3 (Superselect; Merck, Darmstadt, Germany) and 1 mL of 30% H_2O_2 and made up to 10 mL by addition of 50% nitric acid. Blood (max. 380 μL), urine (max. 1 mL), and faeces samples were made up in the same manner. These samples ($n = 1$ for each treatment) were submitted for ICP−MS. The original Gd content data (μg/L) were recalculated as nmol/g tissue or biofluid, without correction for remaining blood, and then scaled proportionally to correspond to a common CA dose of 100 μmol/kg for each animal. For kidney a correction for urine content was not attempted.

ICP−MS. Samples of harvested cells or tissues were digested with 50% concentrated HNO_3 under microwave heating with a Mars 5 apparatus (CEM GmbH, Kamp-Lintfort, Germany). To each sample was added 100 μL of an aqueous solution of rhodium chloride (1 μg/mL) so that Rh-103 could be used as an internal quantification standard. Gd-157 or Gd-160 to Rh-103 ratio measurements were performed by ion-coupled plasma (ICP) mass spectrometry (Finnigan Element 2; Thermo Electron Corp., Bremen, Germany). Over the course of the study, two different instruments were used: instrument 1 for studies with **Gd-1**, **Gd-2**, and **Gd-4** and instrument 2 for all studies with **Gd-3**, **Gd-5**, and **Gd-6**. The gadolinium concentrations in μg/L for the original sample volume were reported as mean and SD of three determinations for each sample using standard curves created prior to the analyses. For instrument 1 the detection threshold was ca. 1 μg/L; instrument 2 provided lower SDs for repeated measures (<3%) and a detection threshold of 0.1 μg/L. For experiments with $n = 1$ sample, SD values represent the variance of the measurement; for $n = 2$ samples, SD represents the sample variance.

Relaxivities of Gd-DTPA-Polyamine Complexes. Relaxation rates R_1 for PBS and 1 mM solutions of **Gd-3**, **Gd-5**, and **Gd-6** were determined at 300.13 MHz and 25 °C using a Bruker AM-300 "super-wide-bore" spectrometer (15-cm vertical magnet bore, 7.05 T) equipped with MR imaging hardware, including a micro-imaging probe with 10 mm rf insert and an actively shielded XYZ field gradient system. The solutions were placed in glass capillaries (1.57 mm i.d.) which were taped to a cardboard holder in a 2×2 array and inserted into an empty 10 mm NMR sample tube. Relaxation data for all four solutions were obtained simultaneously with a saturation−recovery spin−echo imaging sequence (4 mm transverse slice thickness, 16 values of the recovery time). Central regions of interest (ROI, 0.66 mm square) were assigned to each capillary image, the mean ROI signal intensities were corrected for the small contribution from noise in the magnitude-mode image presentation,[43,44] and the corrected data vs recovery time were analyzed by nonlinear least-squares fitting to a three-parameter monoexponential function, as described in detail in the Supporting Information. In a separate experiment under identical conditions, the relaxation rate for a capillary containing 5 mM Gd(DTPA) was determined by a spectroscopic inversion−recovery measurement of signal integrals for 12 recovery times.

Intracellular Relaxivities. MH3924A tumor cells were cultured under the standard conditions described above and incubated at 37 °C for 24 h with the selected CA (**Gd-3**, **Gd-5**, or **Gd-6**) at 0, 10, 30, or 75 μM ($n = 1$ for all incubations). Cells were harvested by trypsination (to remove externally bound CA) and washed three times in ice-cold PBS. Cell pellets containing 4×10^6 cells were taken up in ca. 40 μL of PBS (pH 7.4) and transferred to glass capillaries (1.57 mm i.d.). For each incubation an aliquot of 1.5×10^6 cells was frozen for later determination of the intracellular Gd concentration by ICP−MS. The four capillaries corresponding to different concentrations of a given CA were centrifuged at 800*g* for 2 min to create compact pellets (Heraeus Biofuge 13). The capillaries were placed together in a 2×2 array in an empty 10 mm NMR tube using a cardboard holder. Relaxation rates R_1 at 300.13 MHz and 25 °C were determined by saturation−recovery spin−echo MRI (2 or 3 mm transverse slice through the center of each pellet, 16 values of the recovery time) as described above. A separate series of measurements was performed for each CA. Excellent fits to a monoexponential function were obtained, indicating that intra- and extracellular water were in the fast-exchange limit relative to the difference in their individual relaxation rates. Therefore, the observed relaxation rate can be written as

$$R_{1obs} = f_{in}R_{1in} + (1 - f_{in})R_{1ex} \quad (1)$$

Relaxation rates R_{1in} for intracellular water were calculated assuming two-site fast exchange, $R_{1ex} = 0.337$ (the value for PBS), and a mole fraction for intracellular water, $f_{in} = 0.32$, as determined by Terreno et al.[36] for rat hepatocarcinoma cell pellets. Finally, the molar relaxivities r_{1obs} and r_{1in} were calculated from the differences $R_{1obs} - R^0_{1obs}$ and $R_{1in} - R^0_{1in,}$ where R^0_1 refers to a relaxation rate in the absence of CA, divided by the intracellular Gd concentrations determined by ICP−MS. Complete details of the measurement and analysis techniques are presented in the Supporting Information.

MRI. At 25 days after inoculation with MH3924A cells, tumor diameters were 10−15 mm, and rats were anesthetized by intravenous injection of ketamin (Ketanest, 0.1 mg/g body wt; Parke-Davis, Berlin, Germany). A dose of 100 μmol/kg Gd(DTPA) or Gd(DO3A-butrol) or one of the synthesized agents **Gd-3**, **Gd-5**, or **Gd-6** was injected intravenously into a lateral tail vein. For one experiment a higher dose (360 μmol/kg) of Gd(DTPA) was used. Individual rats were examined by MRI at 1 and 24 h post Gd, in the case of Gd(DTPA) also at ca. 15 min post Gd. Proton imaging studies were performed at 2.35 T (100.3 MHz) with a Biospec 24/40 instrument (Bruker BioSpin MRI, Ettlingen, Germany) using T_2-weighted spin−echo and T_1-weighted gradient-echo techniques. For details, see the Supporting Information.

Acknowledgment. We thank the following colleagues: W. D. Lehmann, Ralf Krüger (DKFZ), and M. Krachler (Univ. of Heidelberg) for ICP−MS analyses; H. Eskerski, K. Leotta, and U. Schierbaum for assistance with the animal experiments; S. Vorwald (Univ. of Heidelberg) for histological preparations; J. Kretschmer (DKFZ) for help with subcellular fractionation.

Supporting Information Available: Detailed analytical data (NMR, MS, HPLC) for the synthesized compounds and a complete description of the MRI techniques and the analysis of relaxation data. This material is available free of charge via the Internet at http://pubs.acs.org.

References

(1) Caravan, P.; Ellison, J. J.; McMurry, T. J.; Lauffer, R. B. Gadolinium(III) chelates as MRI contrast agents: structure, dynamics, and applications. *Chem. Rev.* **1999**, *99*, 2293−2352.

(2) Fulvio, U.; Aime, S.; Anelli, P. L.; Botta, M.; Brochetta, M.; de Haën, C.; Ermondi, G.; Grandi, M.; Paoli, P. Novel contrast agents for magnetic resonance imaging. Synthesis and characterization of the ligand BOPTA and its Ln(III) complexes (Ln = Gd, La, Lu). X-ray structure of disodium (TPS-9−14533.7286-C-S)-[4-carboxy-5,8,11-tris(carboxymethyl)-1-pheny l-2-oxa-5,8,11-triazatridecan-13-oato-(5-)]gadolinate(2-) in a mixture with its enantiomer. *Inorg. Chem.* **1995**, *34*, 633−642.

(3) Ostrowitzki, S.; Fick, J.; Roberts, T. P.; Wendland, M. F.; Aldape, K. D.; Mann, J. S.; Israel, M. A.; Brasch, R. C. Comparison of gadopentetate dimeglumine and albumin-(Gd-DTPA)30 for microvessel characterization in an intracranial glioma model. *J. Magn. Reson. Imaging* **1998**, *8*, 799−806.

(4) Schima, W.; Saini, S.; Petersein, J.; Weissleder, R.; Harisinghani, M.; Mayo-Smith, W.; Hahn, P. F. MR imaging of the liver with Gd-BOPTA: quantitative analysis of T_1-weighted images at two different doses. *J. Magn. Reson. Imaging* **1999**, *10*, 80−83.

(5) Aime, S.; Barge, A.; Cabella, C.; Crich, S. G.; Gianolio, E. Targeting cells with MR imaging probes based on paramagnetic Gd(III) chelates. *Curr. Pharm. Biotechnol.* **2004**, *5*, 509−518.

(6) Artemov, D. Molecular magnetic resonance imaging with targeted contrast agents. *J. Cell Biochem.* **2003**, *90*, 518−524.

(7) Shahbazi-Gahrouei, D.; Rizvi, S. M.; Williams, M. A.; Allen, B. J. In vitro studies of gadolinium-DTPA conjugated with monoclonal antibodies as cancer-specific magnetic resonance imaging contrast agents. *Aust. Phys. Eng. Sci. Med.* **2002**, *25*, 31−38.

(8) Konda, S. D.; Aref, M.; Wang, S.; Brechbiel, M.; Wiener, E. C. Specific targeting of folate-dendrimer MRI contrast agents to the high affinity folate receptor expressed in ovarian tumor xenografts. *MAGMA* **2001**, *12*, 104−113.

(9) Allen, M. J.; MacRenaris, K. W.; Venkatasubramanian, P. N.; Meade, T. J. Cellular delivery of MRI contrast agents. *Chem. Biol.* **2004**, *11*, 301−307.

(10) Allen, M. J.; Meade, T. J. Synthesis and visualization of a membrane-permeable MRI contrast agent. *J. Biol. Inorg. Chem.* **2003**, *8*, 746−750.

(11) Bhorade, R.; Weissleder, R.; Nakakoshi, T.; Moore, A.; Tung, C. H. Macrocyclic chelators with paramagnetic cations are internalized into mammalian cells via a HIV-tat derived membrane translocation peptide. *Bioconjugate Chem.* **2000**, *11*, 301−305.

(12) Prantner, A. M.; Sharma, V.; Garbow, J. R.; Piwnica-Worms, D. Synthesis and characterization of a Gd-DOTA-D-permeation peptide for magnetic resonance relaxation enhancement of intracellular targets. *Mol. Imaging* **2003**, *2*, 333−341.

(13) Jones, S. W.; Christison, R.; Bundell, K.; Voyce, C. J.; Brockbank, S. M.; Newham, P.; Linsay, M. A. Characterization of cell-penetrating peptide-mediated peptide delivery. *Br. J. Pharmacol.* **2005**, *145*, 1093−1102.

(14) Crich, S. G.; Biancone, L.; Cantaluppi, V.; Duo, D.; Esposito, G.; Russo, S.; Camussi, G.; Aime, S. Improved route for the visualization of stem cells labeled with a Gd-/Eu-chelate as dual (MRI and fluorescence) agent. *Magn. Reson. Med.* **2004**, *51*, 938−944.

(15) Young, S. W.; Qing, F.; Harriman, A.; Sessler, J. L.; Dow, W. C.; Mody, T. D.; Hemmi, G. W.; Hao, Y.; Miller, R. A. Gadolinium(III) texaphyrin: a tumor selective radiation sensitizer that is detectable by MRI. *Proc. Natl. Acad. Sci. U.S.A.* **1996**, *93*, 6610−6615. Erratum in *Proc. Natl. Acad. Sci. U.S.A.* 1999, *96*, 2569b.

(16) Heckl, S.; Pipkorn, R.; Waldeck, W.; Spring, H.; Jenne, J.; von der Lieth, CW.; Corban-Wilhelm, H.; Debus, J.; Braun, K. Intracellular visualization of prostate cancer using magnetic resonance imaging. *Cancer Res.* **2003**, *63*, 4766−4772.

(17) Eisenhut, M.; Mohammed, A.; Mier, W.; Schonsiegel, F.; Friebe, M.; Mahmood, A.; Jones, A. G.; Haberkorn, U. Melanoma uptake of ^{99m}Tc complexes containing the *N*-(2-diethylaminoethyl)benzamide structural element. *J. Med. Chem.* **2002**, *45*, 5802−5805.

(18) Friebe, M.; Mahmood, A.; Bolzati, C.; Drews, A.; Johannsen, B.; Eisenhut, M.; Kraemer, D.; Davison, A.; Jones, A. G. [^{99m}Tc]-oxotechnetium(V) complexes amine-amide-dithiol chelates with dialkylaminoalkyl substituents as potential diagnostic probes for malignant melanoma. *J. Med. Chem.* **2001**, *44*, 3132−3140.

(19) Friebe, M.; Mahmood, A.; Spies, H.; Berger, R.; Johannsen, B.; Mohammed, A.; Eisenhut, M.; Bolzati, C.; Davison, A.; Jones, A. G. '3+1′ mixed-ligand oxotechnetium(V) complexes with affinity for melanoma: synthesis and evaluation in vitro and in vivo. *J. Med. Chem.* **2000**, *43*, 2745−2752.

(20) Eisenhut, M.; Hull, W. E.; Mohammed, A.; Mier, W.; Lay, D.; Just, W.; Gorgas, K.; Lehmann, W. D.; Haberkorn, U. Radioiodinated *N*-(2-diethylaminoethyl)benzamide derivatives with high melanoma uptake: structure-affinity relationships, metabolic fate, and intracellular localization. *J. Med. Chem.* **2000**, *43*, 3913−3922.

(21) Wolf, M.; Bauder-Wüst, U.; Mohammed, A.; Schönsiegel, F.; Mier, W.; Haberkorn, U.; Eisenhut, M. Alkylating benzamides with melanoma cytotoxicity. *Melanoma Res.* **2004**, *14*, 353−360.

(22) Michelot, J. M.; Moreau, M. F.; Labarre, P. G.; Madelmont, J. C.; Veyre, A. J.; Papon, J. M.; Parry, D. F.; Bonafous, J. F.; Boire, J. Y.; Desplanches, G. G.; Bertrant, S. J.; Meyniel, G. Synthesis and evaluation of new iodine-125 radiopharmaceuticals as potential tracers for malignant melanoma. *J. Nucl. Med.* **1991**, *32*, 1573−1580.

(23) Michelot, J. M.; Moreau, M. F.; Veyre, A. J.; Bonafous, J. F.; Bacin, F. J.; Madelmont, J. C.; Bussiere, F.; Souteyrand, P. A.; Mauclaire, L. P.; Chossat, F. M.; Papon, J. M.; Labarre, P. G.; Kauffmann, P.; Plagne, R. J. Phase II scintigraphic clinical trial of malignant melanoma and metastases with iodine-123-*N*-(2-diethylaminoethyl 4-iodobenzamide). *J. Nucl. Med.* **1993**, *34*, 1260−1266.

(24) Moreau, M. F.; Papon, J.; Labarre, P.; Moins, N.; Borel, M.; Bayle, M.; Bouchon, B.; Madelmont, J. C. Synthesis, in vitro binding and biodistribution in B16 melanoma-bearing mice of new iodine-125 spermidine benzamide derivatives. *Nucl. Med. Biol.* **2005**, *32*, 377−384.

(25) Tjalve, H.; Nilsson, M.; Henningsson, A. C.; Henningsson, S. Affinity of putrescine, spermidine and spermine for pigmented tissues. *Biochem. Biophys. Res. Commun.* **1982**, *109*, 1116−1122.

(26) Seiler, N.; Delcors, J. G.; Moulinoux, J. P. Polyamine transport in mammalian cells. An update. *Int. J. Biochem. Cell Biol.* **1996**, *28*, 843−861.

(27) Porter, C. W.; Miller, J.; Bergeron, R. J. Aliphatic chain length specificity of the polyamine transport system in ascites L1210 leukemia cells. *Cancer Res.* **1984**, *44*, 126−128.

(28) Seiler, N. Thirty years of polyamine-related approaches to cancer therapy. Retrospect and prospect. Part 2. Structural analogues and derivatives. *Curr. Drug Targets* **2003**, *4*, 565−585.

(29) Pohjanpelto, P. Putrescine transport is greatly increased in human fibroblasts initiated to proliferate. *J. Cell Biol.* **1976**, *68*, 512−520.

(30) Dalla Via, L.; Salvi, M.; Di Noto, V.; Stefanelli, C.; Toninello, A. Membrane binding and transport of *N*-aminoethyl-1,2-diamino ethane (dien) and *N*-aminopropyl-1,3-diamino propane (propen) by rat liver mitochondria and their effects on membrane permeability transition. *Mol. Membr. Biol.* **2004**, *21*, 109−118.

(31) Cullis, P. M.; Green, R. E.; Merson-Davies, L.; Travis, N. Probing the mechanism of transport and compartmentalization of polyamines in mammalian cells. *Chem. Biol.* **1999**, *6*, 717−729.

(32) Holley, J.; Mather, A.; Cullis, P.; Symons, M. R.; Wardman, P.; Watt, R. A.; Cohen, G. M. Uptake and cytotoxicity of novel nitroimidazole-polyamine conjugates in Ehrlich ascites tumor cells. *Biochem. Pharmacol.* **1992**, *43*, 763−769.

(33) Rannard, S. P.; Davis, N. J. The selective reaction of primary amines with carbonyl imidazole containing compounds: selective amide and carbamate synthesis. *Org. Lett.* **2000**, *2*, 2117−2120.

(34) Rozijn, T. H.; van der Sander, B. P.; Heerschap, A.; Creyghton, J. H.; Bovee, W. M. Determination of in vivo rat muscle Gd-DTPA relaxivity at 6.3 T. *MAGMA* **1999**, *9*, 65−71.

(35) Donahue, K. M.; Burstein, D.; Manning, W. J.; Gray, M. L. Studies of Gd-DTPA relaxivity and proton exchange rates in tissue. *Magn. Reson. Med.* **1994**, *32*, 66−76.

(36) Terreno, E.; Crich, S. G.; Belfiore, S.; Biancone, L.; Cabella, C.; Esposito, G.; Manazza, A. D.; Aime, S. Effect of the intracellular localization of a Gd-based imaging probe on the relaxation enhancement of water protons. *Magn. Reson. Med.* **2006**, *55*, 491−497.

(37) Styers, M. L.; Salazar, G.; Love, R.; Peden, A. A.; Kowalczyk, A. P.; Faundez, V. The endo-lysosomal sorting machinery interacts with the intermediate filament cytoskeleton. *Mol. Biol. Cell* **2004**, *15*, 5369−5382.

(38) Zhuo, J.-C.; Cai, J.; Soloway, A. H.; Barth, R. F.; Adams, D. M.; Ji, W.; Tjarks, W. Synthesis and biological evaluation of boron-containing polyamines as potential agents for neutron-capture therapy of brain tumors. *J. Med. Chem.* **1999**, *42*, 1282−1292.

(39) Cabella, C.; Geninatti, Crich, S.; Corpillo, D.; Barge, A.; Ghirelli, C.; Bruno, E.; Lorusso, V.; Uggeri, F.; Aime, S. Cellular labeling with Gd(III) chelates: only high thermodynamic stabilities prevent the cells acting as 'sponges' of Gd^{3+} ions. *Contrast Med. Mol. Imaging* **2006**, *1*, 23−29.
(40) Crich, S. G.; Barge, A.; Battistini, E.; Cabella, C.; Coluccia, S.; Longo, D.; Mainero, V.; Tarone, G.; Aime, S. Magnetic resonance imaging visualization of targeted cells by the internalization of supramolecular adducts formed between avidin and biotinylated Gd^{3+} chelates. *J. Biol. Inorg. Chem.* **2005**, *10*, 78−86.
(41) Saunders, N. A.; Ilett, K. F.; Minchin, R. F. Pulmonary alveolar macrophages express a polyamine transport system. *J. Cell Physiol.* **1989**, *139*, 624−631.
(42) Minchin, R. F.; Raso, A.; Martin, R. L.; Ilett, K. F. Evidence for the existence of distinct transporters for the polyamine putrescine and spermidine in B16 melanoma cells. *Eur. J. Biochem.* **1991**, *200*, 457−462.
(43) Henkelman, R. M. Measurement of signal intensities in the presence of noise in MR images. *Med. Phys.* **1985**, *12*, 232−233.
(44) Bernstein, M. A.; Thomasson, D. M.; Perman, W. H. Improved detectability in low signal-to-noise ratio magnetic resonance images by means of a phase-corrected real reconstruction. *Med. Phys.* **1989**, *16*, 813−817.

JM061003A